Application of the stretched exponential function to fluorescence lifetime imaging of biological tissue

J. Siegel*[a], K.C. Benny Lee[a], S.E.D. Webb[a], S. Lévêque-Fort[a], M.J. Cole[a], R. Jones[a], K. Dowling[a], P.M.W. French[a] and M.J. Lever[b],

[a] Department of Physics, Imperial College;
[b] Department of Biological and Medical Systems, Imperial College

ABSTRACT

The fluorescence decay in fluorescence lifetime imaging (FLIM) is typically fitted to a multi-exponential model with discrete lifetimes. The interaction between fluorophores in heterogeneous samples (e.g. biological tissue) can, however, produce complex decay characteristics that do not correspond to such models. Although they appear to provide a better fit to fluorescence decay data than the assumption of a mono-exponential decay, the assumption of multiple discrete components is essentially arbitrary and often erroneous. The stretched exponential function (StrEF) describes fluorescence decay profiles using a continuous lifetime distribution as has been reported for tryptophan, being one of the main fluorophores in tissue. We have demonstrated that this model represents our time-domain FLIM data better than multi-exponential discrete decay components, yielding excellent contrast in tissue discrimination without compromising the goodness of fit, and it significantly decreases the required processing time. In addition, the stretched exponential decay model can provide a direct measure of the sample heterogeneity and the resulting heterogeneity map can reveal subtle tissue differences that other models fail to show.

Keywords : Continuous lifetime distribution, image processing, tissue discrimination, fluorescence lifetime imaging

1. INTRODUCTION

In fluorescence lifetime imaging (FLIM), the decay in fluorescence intensity across a sample is measured after optical excitation. The fluorescence lifetime contains functional information via its dependence on fluorophore radiative and non-radiative decay rates. This functionality has been exploited to quantify physiological parameters including pH[1,2], $[Ca^{2+}]$[3] and pO_2[4]. Because the fluorescence lifetime is derived from relative intensity values, it can provide useful information concerning biological tissue in spite of the heterogeneity and strong optical scattering. Fluorescence lifetime imaging (FLIM), in which a map of the spatial distribution of fluorophore lifetimes is displayed, thus provides a powerful functional imaging modality for biomedicine.

In our laboratory, time-domain FLIM data are obtained by acquiring a series of time gated intensity maps at increasing delays after ultrashort laser pulse excitation. The series of relative fluorescence intensity values for each pixel in the field of view can then be fitted to an assumed decay model, conventionally a multiple exponential function with discrete lifetimes. In general we have observed that the autofluorescence decays of collagen, elastin and other tissue components do not fit a single exponential decay profile and that the assumption of a double exponential decay provides a better fit[5]. However, an apparently satisfactory fit to such a model, e.g., a double exponential model with discrete lifetimes, can conceal the actual complexity in the decay mechanisms[6]. In particular, interaction between fluorophores in heterogeneous samples can yield complex decay mechanisms that may result in a continuous distribution of fluorescence lifetimes[7]. There are many situations in which one does not expect a limited number of discrete decay times, e.g. for a fluorophore in a mixture of solvents, such that a range of fluorophore environments exists, each environment results in a different intensity decay[8]. For a single-tryptophan protein for instance, the resulting

* j.siegel@ic.ac.uk, phone 44-20-7594 7755; fax 44-20-7594-7782; http://www.photonics.ic.ac.uk/femto/; Department of Physics, Imperial College of Science, Technology and Medicine, Prince Consort Road, London SW7 2BW, U.K.

distribution of protein conformations may lead to a continuous distribution of fluorescence lifetimes[7,9]. Another possibility is a protein that has so many tryptophan residues that it is not practical to consider the individual decay times[8]. Generally, these variations are present on a molecular scale and therefore cannot be spatially resolved. In these cases, fitting to a double-exponential model would imply an erroneous assumption of two discrete lifetimes, which may lead to image artifacts in the FLIM maps obtained. Although it would provide a better fit than the single-exponential, due to the extra two fitting parameters, its use cannot be justified from a physical point of view. Similarly, triple- or higher exponential decay models will improve the goodness of fit solely by the extra fitting parameters and not due to a better description of the experimental decay dynamics.

The stretched exponential function[10], also known as the Kohlrausch-Williams-Watts function,

$$I(t) = I_0 \exp\left[-\left(\frac{t}{\tau_{kww}}\right)^{1/h}\right] \tag{1}$$

is proposed here as an alternative model to fit complex fluorescence decay profiles in biological tissue. This function, which has previously been applied to magnetic resonance imaging data[11], can describe decay profiles using a continuous lifetime distribution. Our motivation to apply it to FLIM is triggered by the fact that - from a mathematical point of view – the stretched exponential decay can be expressed as a continuous distribution of lifetimes[12]

$$I(t) = \int_0^\infty \exp\left(-\tfrac{t}{\tau}\right)\rho(\tau)d\tau \tag{2}$$

as it can be found in heterogeneous samples. The StrEF should therefore be more appropriate to describe the decay in heterogeneous tissue samples showing continuous lifetime distributions rather than multi-exponential models with an arbitrary number of discrete lifetimes. We have applied the StrEF to whole-field FLIM and demonstrate that this decay model yields strong contrast in tissue discrimination, without compromising the goodness of fit and without need for an arbitrary assumption on the number of fluorophores present, while it significantly decreases the required processing time.

2. SIMULATIONS

The mathematical equivalence between the StrEF (eq. 1) and the expression for the continuous lifetime distribution (eq. 2) was tested by way of a simulation. Sets of multi-exponential data that included an element of Poisson noise were simulated using

$$I = \sum_{j=1}^{J} \alpha_j \exp\left(-\frac{t}{\tau_j}\right) + Poisson\ noise \tag{3}$$

where τ_j values are lifetimes chosen to emulate experimental values, α_j values are the fractional contribution of each of these components and J determines the total number of exponential terms used for simulating a particular set of data. Fig. 1(a) illustrates the degree to which the stretched exponential function fits simulated multiple exponential decay profiles. The goodness of fit used was the statistical χ^2/(degrees of freedom), defined as:

$$\frac{\chi^2}{(dof)} = \frac{1}{N-m}\sum_{i=1}^{N}\frac{[I_i - I(t_i)]^2}{\sigma_i^{\,2}} \tag{4}$$

where t_i, I_i values are the pairs of N data points, σ_i values are the expected standard deviation of the data points and m is the number of fitting parameters. An ideal fitting model will be indicated by a value of one for χ^2/(degrees of freedom).

It can be seen from Fig. 1(a) that the stretched exponential function becomes a better fitting model as the number of exponential terms increases*, approaching ideality as the number tends to infinity. This confirms the mathematical equivalence between the StrEF (eq. 1) and the expression for the continuous lifetime distribution (eq. 2).

---

* *An exception exists when only one exponential term is used for the simulation, in which case the stretched exponential model fits the simulated data ideally with h=1.*

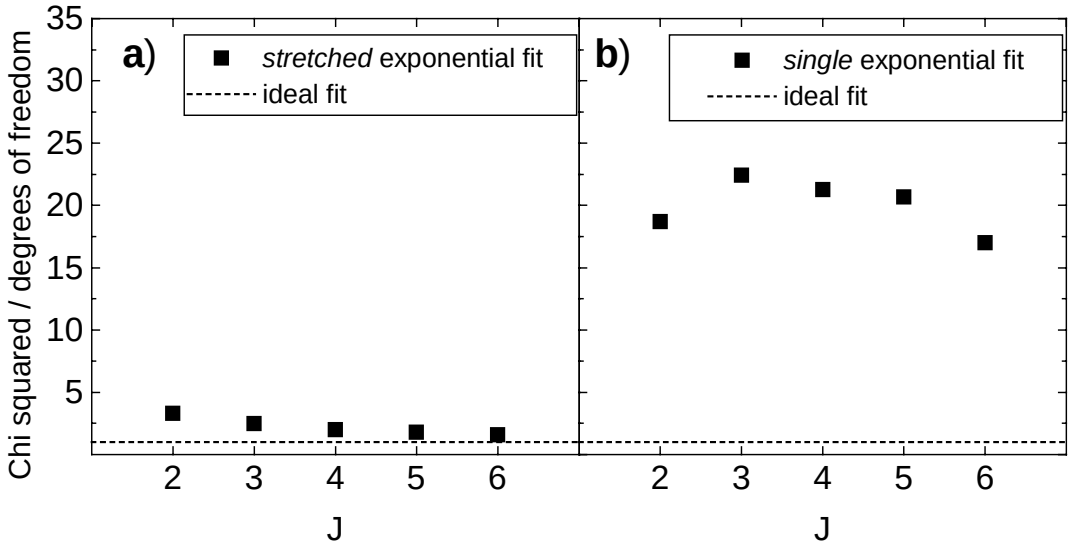

Fig. 1: Performance of (a) the stretched exponential function and (b) the single exponential function in describing multi-exponential decay data.

In order to get a more quantitative impression of the goodness of fit when using a StrEF to fit multi-exponential data, the data was also fitted to a single exponential function and this is shown in Fig. 1(b). It can be seen that all single exponential fits to multiple exponential data were equally unreliable (χ^2/dof ~ 20), independent of J. For the same set of data, the stretched exponential model yields a considerably better goodness of fit even for the case of its "worst performance": the double exponential decay (χ^2/dof < 3.5). Also here, from a practical point of view, an important conclusion can be drawn because a single exponential model is commonly used in FLIM as a first guess due to the short calculation time. The comparison of the Figs. 1 (a) and 1 (b) suggests that the use of the StrEF provides a dramatically better fit to multi-exponential decays than a single exponential fit without an excessive increase in calculation time (only a factor of about 1.5). It is worth noting that, even in the case of a purely single-exponential decay, the StrEF gives the correct result since this corresponds to its degenerate form with $h = 1$.

So far, we have considered the performance of the StrEF on simulated decay data that are purely multi-exponential. Experimental fluorescence decay profiles, however, are often *not* multi-exponential decays. As pointed out before, a multi-exponential model neglects the interaction between fluorophores and their environment in complex samples like biological tissue, which yields continuous distributions rather than a few discrete lifetimes. In the following we have studied the performance of the StrEF in fitting real whole-field FLIM data of rat tissue.

3. EXPERIMENT

Our time-domain FLIM apparatus and the data acquisition schema are shown in Fig. 2. The excitation source is a commercial ultrafast Ti:Sapphire laser oscillator (Spectra-Physics Tsunami), the output of which is amplified in a home-built Cr:LiSAF regenerative amplifier pumped by the same argon-ion laser as the oscillator. This produces pulses of ~ 10 μJ energy and 10 ps duration at 5 kHz repetition rate at ~ 830 nm. These pulses are then frequency doubled to produce a 1 μJ whole-field excitation source at 415 nm for the tissue sample. The spatial intensity distribution of the tissue autofluorescence is imaged onto a gated optical intensifier (Kentech Instruments Ltd), which acquires whole-field 2D intensity images with an effective gate width of ~ 90ps including timing jitter. FLIM maps are produced by acquiring a series of time-gated fluorescence intensity images at a range of time delays after excitation and, for each pixel in the field of view, fitting the assumed decay profile using the Marquardt algorithm for nonlinear least squares fits. When applied to simple fluorophore distributions, this instrument can provide FLIM maps with an update time of only 3 seconds[13] and resolve lifetime differences of < 10 picoseconds[5].

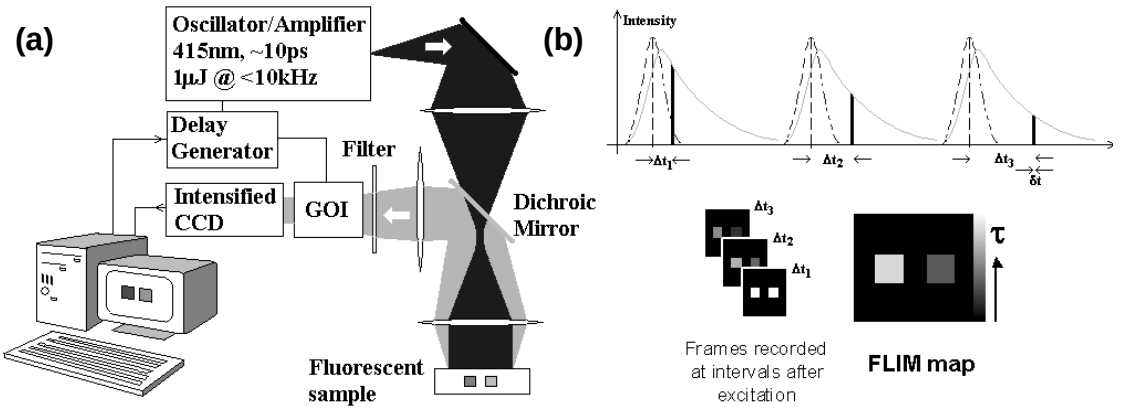

Fig. 2: (a) Schematic of the experimental FLIM system and (b) the acquisition process.

In this work we compare FLIM maps obtained using single, double and stretched exponential fits. In the case of the single exponential fit, the lifetime τ is used as the plotting parameter on a greyscale map for display. In the case of the double exponential fit, the short (τ_1) and the long (τ_2) lifetime components are used. In the case of the stretched exponential function, it is necessary to interpret the lifetimes in a statistical manner in order to correctly describe a decay given by Eq. 1 and 2. One possibility of such a statistical interpretation of the continuous lifetime distribution is the 95-percentile lifetime. We have chosen to work with the mean lifetime $<\tau>$ of the distribution that is directly obtained from the integration of Eq. 1, given by

$$\langle \tau \rangle = h\tau_{kww}\Gamma[h] \tag{5}$$

where $\Gamma[h]$ is the gamma function. Unlike multi-exponential models, the StrEF offers a further parameter of potential interest: the heterogeneity parameter *h*. This parameter is related to the stretching of the decay process and a direct measure of the width of the lifetime distribution. In addition to the mean lifetime $<\tau>$ as a plotting parameter, we have therefore also plotted *h* on a greyscale map.

4. RESULTS

We have investigated tissue components, such as collagen and elastin, which were extracted from rat. The elastin was obtained by hydrolyzing aorta. For excitation at 415 nm, collagen and elastin have similar fluorescence spectra but they may be successfully contrasted using fluorescence lifetime[5]. The fluorescence observed for this excitation wavelength is attributed to the cross-linkages in collagen and elastin[14]. Like single-tryptophan proteins[7] - which are considered the major fluorophores for excitation in the UV[15] - we also expect elastin and collagen to show continuous lifetime distributions rather than a few discrete lifetimes due to a range of micro-environments. Therefore, the choice of the decay model (i.e., whether it is a single, double or stretched exponential decay) was expected to impact the specificity of tissue discrimination and the quality of the FLIM images. Fig. 3 shows FLIM maps of collagen, aorta and elastin excited at 415 nm obtained by single, double and stretched exponential decay models. The lifetime ranges have been scaled to minimize any unnecessary cropping of the deduced lifetimes. In Fig. 3a, the short-lived component (τ_1) of the double exponential decay can be seen, which does not show any significant contrast between the different tissues. The longer-lived component (τ_2), although distinguishing the collagen and elastin, only shows a slight difference in lifetime between elastin and aorta (Fig. 3b). In both cases the FLIM maps are relatively noisy since the fluorescence decay is separated into two components, which reduces the S/N ratio of the individual components.

In Fig. 3c it can be seen that a single exponential fit yields a better contrast between the different tissue constituents than the individual components of the double exponential fit. Concerning the stretched exponential fit, Fig. 3d demonstrates that plotting the physically more representative parameter $<\tau>$ also provides strong contrast. In addition, the map of the heterogeneity parameter *h* (Fig. 3e) shows a local inhomogeneity in the collagen where *h* has a very low value, corresponding to a narrower lifetime distribution than the surrounding area. Such additional detail revealed by the heterogeneity parameter may be useful in distinguishing local differences in protein conformations.

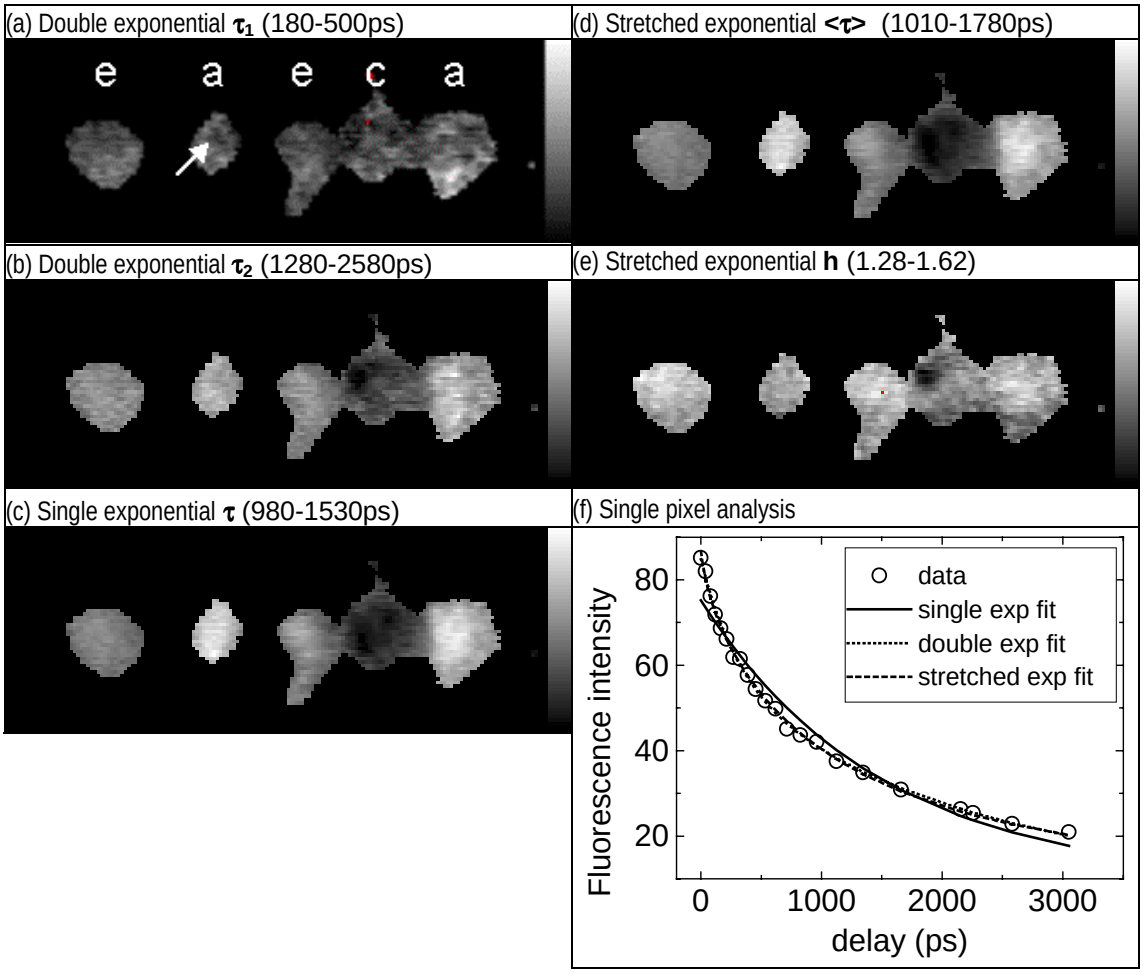

Fig. 3: FLIM maps of aorta – a, collagen – c, elastin – e. (a) Short-lived and (b) long-lived lifetime components of the double exponential model; (c) lifetime for the single exponential model; (d) mean lifetime and (e) heterogeneity parameter for the stretched exponential model. The lifetime and heterogeneity gray scale span over the range given in each individual map, where black represents low lifetime (heterogeneity) values and white high lifetime (heterogeneity) values. The arrow in (a) indicates the coordinates of the single pixel analysis (f).

In order to further assess the different fitting models, we have plotted a typical data set for a single pixel in the field of view (indicated by an arrow in Fig. 3a) together with the corresponding fitted curves (Fig. 3f). We observe that the single exponential model provides a poor fit to the data, despite the fact that it yields a FLIM map with good contrast. This means that the use of a single-exponential model yields incorrect absolute values of the lifetime data but is nonetheless sensitive to spatial variations in fluorescence lifetime. On the other hand, the double exponential model provides a satisfyingly good fit to the data but the plotting of the individual lifetime components yields poor contrast in the FLIM map. The stretched exponential model, however, provides both a satisfyingly good fit to the data (Fig. 3f) and good contrast when plotting $<\tau>$ (Fig. 3d). This suggests that the StrEF is the most appropriate model to distinguish different tissue constituents.

We have also applied the different decay models to whole-field FLIM data of unstained rat tissue sections. For comparison, Fig. 4(a) shows a commercial light microscope image of a stained tissue section from a rat's ear, highlighting two veins, an artery, cartilage and some hair. The corresponding FLIM maps of a similar but unstained section obtained using our home-built laboratory FLIM microscope are shown in Fig. 4(b)-(f). When fitting to a double-exponential decay, we again find that the FLIM maps of the individual “discrete” components (Fig. 4b,c) exhibit

relatively poor contrast and spatial image quality due to the reduced S/N ratio. On the other hand, the stretched exponential function based on a continuous lifetime distribution does represent the likely physical origin of the observed fluorescence decay profiles and the FLIM map of $<\tau>$ from the StrEF (Fig. 4e) exhibits excellent contrast and spatial image quality. In particular, we find a strong contrast between elastic cartilage, the surrounding tissue, blood containing vessels and even the vessel walls are clearly contrasted. In addition, the StrEF provides additional information about the sample *heterogeneity* through the map of the parameter *h* (Fig. 4f). For this tissue section, all the biological structures in the section exhibit a similar low heterogeneity value except the veins and arteries, which exhibit relatively high values. Since these vessels retained blood that had clotted post mortem, we believe that the high h-values are characteristic of clotted blood. This significant difference in the h-values between the blood-containing vessels and the surrounding tissue provides an even better contrast than that obtained by plotting lifetime values. Thus it becomes possible to identify other, much smaller regions of clotted blood, such as the one located to the right of the upper vein.

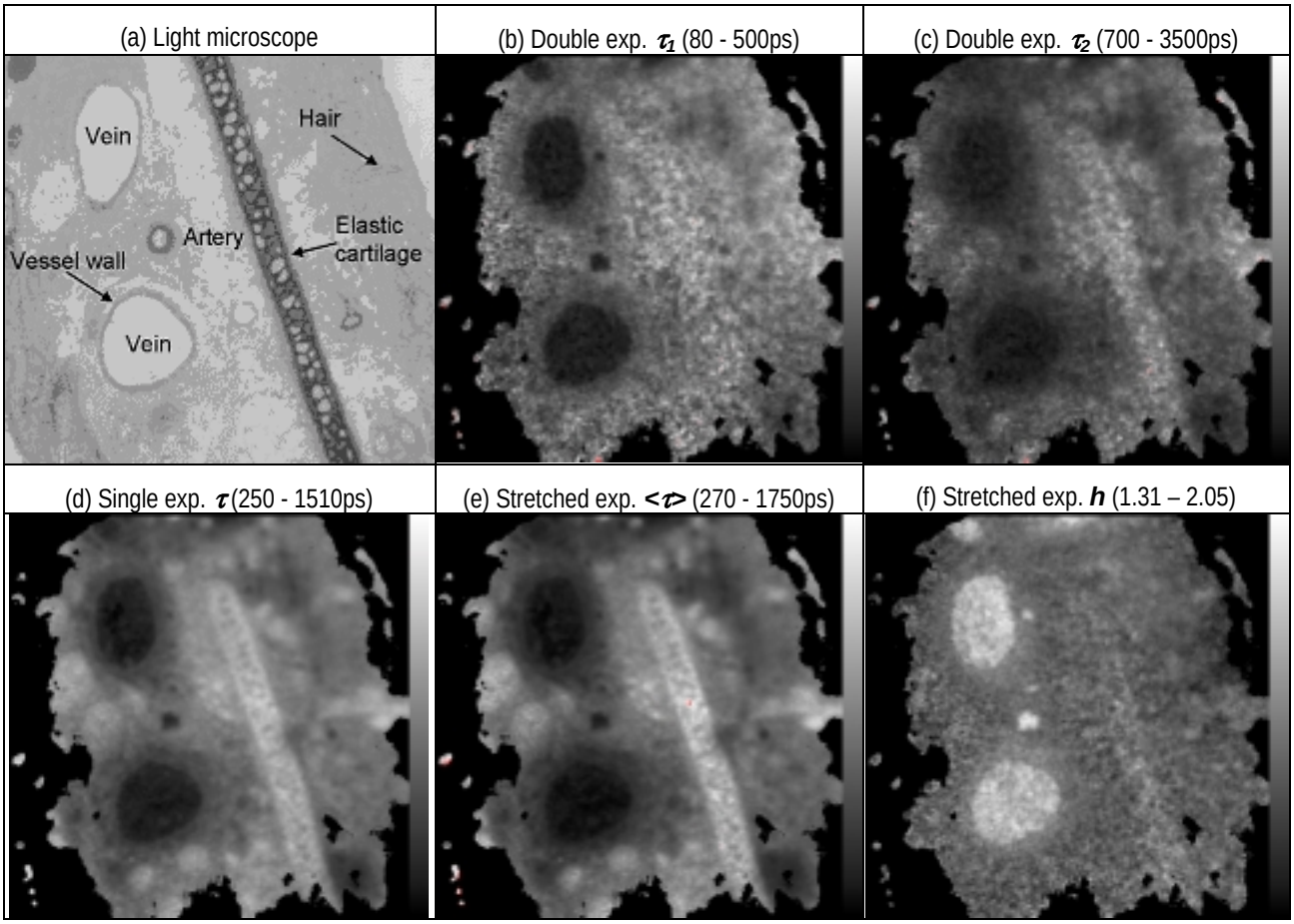

Fig. 4: (a) A light microscope image of a stained tissue section from a rat's ear. The corresponding FLIM maps from a similar unstained tissue section as obtained with our FLIM apparatus are shown for (b) the short-lived and (c) the long-lived lifetime components of the double exponential model; (d) the lifetime for the single exponential model; (e) the mean lifetime and (f) the heterogeneity parameter for the stretched exponential model. The lifetime and the heterogeneity grey scale span over the range given in each individual map.

We note that the fluorescence lifetime map obtained using a single exponential function (Fig. 4d) shows contrast and spatial quality that are comparable to the lifetime map obtained with the stretched exponential model (Fig. 4e). However, analysis of the goodness of fit for the data from a typical pixel confirmed a much better fit for the stretched exponential model (data not shown), as already observed in Fig. 3f.

5. DISCUSSION

The use of the stretched exponential function for analysing fluorescence decay profiles has been shown to provide excellent tissue discrimination and spatial image quality in whole field FLIM maps. Even more importantly, the stretched exponential function not only describes the decay profiles almost exactly, but is also derived from the more realistic decay model of continuous lifetime distributions in biological tissue, rather than from an arbitrary assumption of single or multiple discrete exponential decay components. This has the potential of revealing subtle differences in fluorescence decay profiles, possibly improving the specificity of FLIM. Moreover, this new approach yields, besides the mean lifetime $<\tau>$ of the distribution, an additional parameter of interest (h), which is related to the width of the lifetime distribution and which is a direct measure of the local heterogeneity of the sample. The heterogeneity parameter is important because it enables the study of mechanisms that cause a continuous lifetime distribution to broaden or narrow. Future work on a variety of different tissue types and in different environmental conditions will hopefully provide more insight in this matter.

Most previous investigations of the autofluorescence of tissue have used excitation wavelengths in the UV[16], for which the major fluorophores are tryptophan and NADH, although there is also fluorescence observed from elastin and collagen[15]. Work done with longer wavelength UV excitation has shown that, for excitation at 310/312nm, the effect of the fluorescence of tryptophan is minimized[15] and that most of the observed fluorescence is due to elastin and collagen. The rejection of tryptophan will be even greater at the excitation wavelength used in our study (415 nm) and so we attribute most of the fluorescence observed in these experiments to elastin and collagen. While continuous distributions of lifetimes in proteins have been found so far only for tryptophan[7], our work is consistent with elastin and collagen also exhibiting stretched exponential fluorescence decay profiles and continuous lifetime distributions. The macromolecular aggregates that make up tissue fibres are formed by cross-linking between individual protein molecules. Such linkages, when excited at 415nm, are the source of the fluorescence of these materials[14]. The cross-linking occurs outside the cell and varies considerably with factors such as age and the local chemical environment. This variation could be the origin of the broadening of discrete lifetime values in a molecular microenvironment that cannot be resolved spatially.

We note that there is ongoing discussion concerning whether proteins show distributions of lifetimes or discrete components. Vix *et al.*[17] report that the width of lifetime distributions of various single-tryptophan proteins is relatively small (a width of 1.4 ns FWHM with a center lifetime of 7 ns for instance). For this reason they favor discrete components over distributions, as opposed to other authors[9] who work with continuous distributions. Even if one considers such a width/center ratio small enough to be negligible, which we believe is not obvious, one has to remember that the findings of Vix *et al.* apply to each individual distribution of a pure single-tryptophan residue protein. In the complex biological tissues discussed here, however, the expected lifetime distribution should be given by the sum of the distributions of a range of fluorophores and so should be rather broader.

Although the use of the StrEF in this work does not require the determination of the distribution of lifetimes $\rho(\tau)$ (see eq. 2), once determined, the first moment of this distribution corresponds to the mean lifetime $<\tau>$ given in Eq. 5. Other moments of the distribution could be of interest as alternative plotting parameters, potentially providing additional contrast in FLIM maps as already done by the heterogeneity parameter. A reliable algorithm to obtain $\rho(\tau)$ has proven to be the CONTIN program[18] and we have begun to implement the corresponding algorithm in FLIM analysis.

Due to the equivalence between the time-domain and frequency-domain FLIM, it is expected that the stretched exponential model can also give substantial improvement to frequency-domain analysis. However, there is no analytical expression for its Fourier transform because of the unusual mathematical behaviour of the stretched exponential function. Numerical approximations to the frequency-domain description of the stretched exponential model have had limited success due to problems originating from cut-off effects. However, a close relationship has been found between the stretched exponential in the time-domain and the Havriliak-Negami function (HNF) in the frequency-domain. The exact relationship between both functions has been studied and tested for relaxation experiments by Alvarez et al who found a simple relation between the parameters of both functions[12]. The authors concluded that this simple relation is expected to hold for all data that can be described either by the StrEF or the HNF. We think that verification of this prediction would be important since the HNF could provide a potentially useful tool for the frequency-domain FLIM community, complementing the application of the StrEF in the time-domain.

From a computational point of view, the stretched exponential model is highly economical because fewer parameters are needed compared to double- or multi-exponential decay models. This results in significantly faster

image processing of FLIM data. It was observed that the time necessary for processing images using the stretched exponential model was significantly less than that for the double exponential model, even though both yielded similar goodness of fit. As a comparison, for the FLIM maps of the rat's ear image (Fig. 4) the double exponential fit took ~1.5× more processing time than the stretched exponential fit to the same data. This was mainly caused by the larger amount of computational iterations necessary for the double exponential model (6,447,720 iterations), as compared to the stretched exponential model (2,585,025 iterations). This difference in processing speed will be even more pronounced between the stretched exponential model and higher multiple exponential models. For instance, fitting the data of Fig. 4 to a triple exponential model (not shown) took ~11× more processing time than the stretched exponential fit.

A further advantage of the stretched exponential model is that it describes fluorescence decay data without the need for making assumptions about the decay (e.g. number of discrete exponential components in a multiple exponential model), thus making it suitable for fitting fluorescence data with unknown decay characteristics. Even for the analyses of samples other than tissue, which have many lifetime components, the StrEF may be more suitable than conventional multiple exponential models due to the short processing time combined with low deviation from the ideal fit, as evident from Fig. 1.

6. CONCLUSION

Fluorescence lifetime measurements are potentially non-invasive and allow both the identification of specific fluorophores and the quantitative monitoring of their local environment for biomedical imaging. We have demonstrated that the stretched exponential model can represent the observed autofluorescence decay profiles in biological tissue very accurately, yielding excellent contrast and spatial image quality for time domain FLIM maps. This observation is in agreement with earlier suggestions that the complexities in decay mechanisms for fluorescence of tissue proteins like tryptophan lead to continuous distributions of lifetimes rather than a few discrete lifetime components and so the StrEF is therefore more realistic than a single- or double-exponential decay model. Due to the relatively long excitation wavelength used in our experiments, the main tissue fluorophores excited are elastin and collagen, rather than tryptophan, but our results suggest that elastin and collagen also exhibit continuous lifetime distributions well represented by a stretched exponential decay function. The use of such a single generalized decay model also minimizes the processing time and eliminates the need for any presumptive choices on the number of exponential terms currently made when using multiple exponential models. This is especially useful in non-invasive biomedical imaging that utilizes the autofluorescence of endogenous fluorophores in tissues, because no *a priori* knowledge of the decay characteristics is required. Besides the mean lifetime $<\tau>$ of the continuous lifetime distribution, the stretched exponential model provides the additional parameter h which is a direct measure for the local heterogeneity of the sample. This heterogeneity parameter should permit the study of mechanisms that broaden the lifetime distributions in complex samples and it also provides a further means to contrast different biological components.

ACKNOWLEDGEMENTS

The authors wish to thank Jonathan Jones from the Oxford Centre for Quantum Computation for his suggestion to apply the stretched exponential function to FLIM. We also thank Klaus Suhling from the Chemistry Department at Imperial College and Fernando Alvarez from the University in San Sebastian, Spain, for helpful comments. This research was funded by the UK Engineering and Physical Sciences Research Council (EPSRC) and the Biotechnology and Biological Sciences Research Council (BBSRC). K.C.B.L. acknowledges a scholarship awarded by the Public Service Commission (Singapore); M.J.C. and K.D. acknowledge EPSRC CASE studentships with the Institute of Cancer Research at the ICR/Royal Marsden National Hospital trust and S.E.D.W. acknowledges an EPSRC studentship.

REFERENCES

1. R. Sanders, A. Draaijer, H.C. Gerritsen, P.M. Houpt, Y.K. Levine, "Quantitative pH imaging in cells using confocal fluorescence lifetime imaging microscopy", *Anal. Biochem.* **227**, pp. 302-308, 1995.
2. H. Szmacinski, J.R. Lakowicz, "Optical measurements of pH using fluorescence lifetimes and phase-modulation fluorometry", *Analytical Chemistry*, **13**, pp. 1668-1674, 1993.
3. J.R. Lakowicz, H. Szmacinski, K. Nowaczyk, "Fluorescence Lifetime Imaging", *Analytical Biochemistry* **202**, pp. 316-330, 1992.
4. S.B. Bambot, G. Rao, M. Romauld, G.M. Carter, J. Sipior, E. Terpetchnig, and J.R. Lakowicz, "Sensing oxygen through skin using a red diode laser and fluorescence lifetimes", *Biosensors & Bioelectronics* **10**, pp. 643-652, 1995.
5. K. Dowling, M.J. Dayel, M.J. Lever, P.M.W. French, J.D. Hares, A.K.L. Dymoke-Bradshaw, "Fluorescence lifetime imaging with picosecond resolution for biomedical applications", *Opt. Lett.* **23**, pp. 810-812, 1998.
6. D.R. James, W.R. Ware, "A fallacy in the interpretation of fluorescence decay parameters", *Chem. Phys. Lett.* **120**, pp. 455-459, 1985.
7. J.R. Alcala, E. Gratton, and F.G. Prendergast, "Fluorescence lifetime distributions in proteins", *Biophys. J.* **51**, pp. 597-604, 1987.
8. J. R. Lakowicz, *Principles of fluorescence spectroscopy*, 2nd ed., Kluwer Academic/Plenum Publishers, New York, 1999.
9. J.R. Alcala, "The effect of harmonic conformational trajectories on protein fluorescence and lifetime distributions", *J. Chem. Phys.* **101**, pp. 4578-4584, 1994.
10. for instance J.C. Phillips, "Stretched exponential relaxation in molecular and electronic glasses", *Rep. Prog. Phys.* **59**, pp. 1133-1207, 1996.
11. L.a. Morozova_Roche, J.A. Jones, W. Noppe, and C.M. Dobson, "Independent Nucleation and Heterogeneous Assembly of Structure During Folding of Equine Lysozyme, J. Mol. Biol. 289, pp. 1055-1073, 1999.
12. F. Alvarez, A. Alegría, and J. Colmenero, "Relationship between the time-domain Kohlrausch-Williams-Watts and frequency-domain Havriliak-Negami relaxation functions", *Phys. Rev. B* **44**, pp. 7306-7312, 1991.
13. K. Dowling, M.J. Dayel, S.C.W. Hyde, P.M.W. French, M.J. Lever, J.D. Hares, A.K.L. Dymoke-Bradshaw, "High resolution time-domain fluorescence lifetime imaging for biomedical applications", *J. Mod. Opt* **46**, pp. 199-209, 1999.
14. S. Pongor, P.C. Ulrich, F.A. Bencsath and A. Cerami, "Aging of proteins - isolation and identification of a fluorescent chromophore from the reaction of polypeptides with glucose", *Proc. Nat. Ac. Sc. USA - Biol. Sc.* **81**, pp. 2684-2688, 1984.
15. J.J. Baraga, R.P. Rava, M. Fitzmaurice, L.T. Tong, P. Taroni, C. Kittrell, and M.S. Field, "Characterisation of the fluorescent morphological structures in human arterial wall using ultra-violet excited multispectrofluorimetry", *Atherosclerosis*, **88**, pp. 1-14, 1991.
16. H. Zeng, C. Mac Aulay, B. Palcic and D.I. McLean, "A computerised autofluorescence and diffuse reflectance spectroanalyser system for in vivo skin studies", *Phys. Bio. Med.* **38**, pp. 231-240, 1993.
17. A. Vix and H. Lami, "Protein Fluorescence Decay: Discrete Components or Distribution of Lifeitmes? Really no Way Out of the Dilemma?" *Biophys. J.* **68**, pp. 1145-1151, 1995.
18. S.W. Provencher, "CONTIN: A general purpose constrained regularization program for inverting noisy linear algebraic and integral equations", *Comput. Phys. Commun.* **27**, pp. 229-242, 1982.